Molecular Systems Biology 5; Article number 288; doi:10.1038/msb.2009.44
Citation: ***Molecular Systems Biology*** **5:288**

www.molecularsystemsbiology.com

molecular systems biology

Coordinated posttranscriptional mRNA population dynamics during T-cell activation

Neelanjan Mukherjee[1,2,3], Patrick J Lager[1,3], Matthew B Friedersdorf[1], Marshall A Thompson[1,2] and Jack D Keene[1,2,*]

[1] Department of Molecular Genetics and Microbiology, Duke University Medical Center, Durham, NC, USA and [2] University Program in Genetics and Genomics, Duke University Medical Center, Durham, NC, USA
[3] These authors contributed equally to this work
* Corresponding author: Department of Molecular Genetics and Microbiology, Duke University Medical Center, 414 Jones Building Box 3020 DUMC, Durham, NC, 27710, USA. Tel.: +1 919 684 5138; Fax: +1 919 684 8735; E-mail: keene001@mc.duke.edu

Received 11.12.08; accepted 3.6.09

Although RNA-binding proteins (RBPs) coordinate many key decisions during cell growth and differentiation, the dynamics of RNA–RBP interactions have not been extensively studied on a global basis. We immunoprecipitated endogenous ribonucleoprotein complexes containing HuR and PABP throughout a T-cell activation time course and identified the associated mRNA populations using microarrays. We used Gaussian mixture modeling as a discriminative model, treating RBP association as a discrete variable (target or not target), and as a generative model, treating RBP-association as a continuous variable (probability of association). We report that HuR interacts with different populations of mRNAs during T-cell activation. These populations encode functionally related proteins that are members of the Wnt pathway and proteins mediating T-cell receptor signaling pathways. Moreover, the mRNA targets of HuR were found to overlap with the targets of other posttranscriptional regulatory factors, indicating combinatorial interdependence of post-transcriptional regulatory networks and modules after activation. Applying HuR mRNA dynamics as a quantitative phenotype in the drug-gene-phenotype Connectivity Map, we identified candidate small molecule effectors of HuR and T-cell activation. We show that one of these candidates, resveratrol, exerts T-cell activation-dependent posttranscriptional effects that are rescued by HuR. Thus, we describe a strategy to systematically link an RBP and condition-specific posttranscriptional effects to small molecule drugs.
Molecular Systems Biology 5: 288; published online 28 July 2009; doi:10.1038/msb.2009.44
Subject Categories: functional genomics; RNA
Keywords: Connectivity Map; protein–RNA interactions; ribonomics; RNA dynamics; RNA regulons; small molecule drugs

Introduction

RNA-binding proteins (RBPs) and non-coding RNAs are post-transcriptional regulatory factors (PTRFs) that control the fate of each mRNA species. Remodeling of multi-component ribonucleoprotein (RNP) complexes through dynamic interactions between PTRFs and mRNAs results in the coordination of posttranscriptional events, including splicing, export, localization, stability, and translation (Keene, 2007). Regardless of the complex patterns of transcription, integration of the multiple layers of gene expression is ultimately determined at the level of translation. Therefore, global investigation of RNPs and their remodeling is critical for understanding the coordination and control of gene expression.

Transcriptomics (profiling RNA expression levels) does not discriminate between the various states in which each single copy of an mRNA can exist within the ribonome. We define the ribonome as the full complement of molecular interactions among proteins and RNAs within the post-transcriptional environment (Keene, 2001). The 'state' of an mRNA can be defined as a function of its association with one or more PTRFs that affect every aspect of the life of an mRNA. Further, it is impossible to directly detect the changes in the proportion of mRNA existing in a given functional state by solely measuring the changes in mRNA abundance. As RNP complexes are sites that dictate post-transcriptional coordination and control of gene expression,

it is crucial to evaluate the states of mRNA with regards to their associations with RBPs in these complexes under a given condition.

A strategy developed in our laboratory, termed 'ribonomics,' identifies and characterizes protein–RNA interactions of endogenous RNP complexes *en masse* using a method called RIP chip (*r*ibonucleoprotein *i*mmuno*p*recipitation microarray). Ribonomic analysis has been used to discover *cis*-elements (Gerber *et al*, 2004; Lopez de Silanes *et al*, 2004; Morris *et al*, 2008) used by RBPs in *trans*, and data from ribonomic studies show a modular organization (Tenenbaum *et al*, 2000; Gerber *et al*, 2004; Hogan *et al*, 2008; Morris *et al*, 2009) of posttranscriptional networks. This functional organization at the RNA level gave rise to the posttranscriptional RNA operon concept in which functionally related mRNAs are dynamically and coordinately regulated temporally and spatially through RNP-driven mechanisms that involve RBPs and non-coding RNAs (Keene and Tenenbaum, 2002; Keene and Lager, 2005; Keene, 2007).

Although messenger RNP complexes are highly dynamic cellular environments (Brengues *et al*, 2005), very few studies have focused on global RNA dynamics of RNPs across different physiological conditions (Tenenbaum *et al*, 2000; Mazan-Mamczarz *et al*, 2008a, b). Even though ribonomic profiling has been widely used to identify mRNAs associated with a given RBP (Keene, 2007; Halbeisen *et al*, 2008), the overwhelming majority of these studies used RIP-chip experiments from a single condition of growth or perturbation. This is in part because of the lack of analytical approaches for modeling RIP-chip data to determine targets and assign values of condition-specific RNP association that allow systematic comparisons across physiological conditions. Therefore, the development of probabilistic models of RNP association will allow a more thorough and systematic investigation of the contribution of RNP dynamics to the molecular networks activated during development or in response to perturbations.

Among the most extensively studied RNA regulatory elements are the AU-rich elements (AREs), which are the sequences of character that function as instability elements. AREs are found in the 3′ untranslated region (UTR) of mRNAs encoding many immediate early genes, inflammatory cytokines, and growth factors. A group of RBPs, collectively known as ARE-RBPs, are typically negative regulators of the stability and translation of ARE-containing mRNAs. In contrast, members of the ELAV/Hu family of ARE-RBPs, including HuR, have been shown to stabilize and promote translation of mRNAs through interactions with AREs (Levine *et al*, 1993; Jain *et al*, 1997; Fan and Steitz, 1998). However, HuR has been shown to negatively regulate a few target mRNAs (Katsanou *et al*, 2005). Therefore, understanding the interaction dynamics between these functionally diverse ARE-RBPs and their associated ARE-containing mRNAs will be necessary to identify factors controlling the expression of many cytokines and growth factors.

Global studies of T-cell activation, a model for the engagement of the T-cell receptor (TCR) complex by presented antigens, have shown extensive posttranscriptional regulation, specifically alteration of mRNA stability (Lam *et al*, 2001) and alternative splicing (Ip *et al*, 2007). One study found that more than half of the transcriptomic changes that occur during T-cell activation are regulated at the level of mRNA stability and not accompanied by any transcriptional change (Cheadle *et al*, 2005). Furthermore, HuR (Atasoy *et al*, 1998) and ARE containing mRNAs (Shaw and Kamen, 1986), many of which are critical immune regulators, respond dynamically during T-cell activation. For example, engagement of LFA-1, a β_2 integrin that is important for TCR complex signaling, results in HuR nuclear export and stabilization of cytokine mRNAs (Wang *et al*, 2006).

In this study, ribonomic analysis of the RBPs HuR and PABP in mitogen-induced activation of Jurkat T cells was used to achieve the following: (1) probabilistic mixture modeling of condition-specific association for an mRNA with the RNP being interrogated by RIP chip, (2) investigation of the functional relationships and dynamics among RNP-associated mRNAs, (3) usage of RNP dynamics as a quantitative phenotype to identify and validate small molecule drugs that mechanistically modulate RBP states. The results of this study advance our understanding of the mechanisms that underlie global posttranscriptional coordination and control of RNP-driven modules consisting of functionally related mRNAs important for determining phenotypic outcomes in this model system.

Results

Global identification of HuR-associated mRNAs during T-cell activation

We used our established RIP-chip protocol to identify the mRNAs associated with RNP complexes (Figure 1A) containing the RBPs HuR and PABP at 0, 4, and 12 h post-activation of Jurkat cells with phorbol 12-myristate 13-acetate (PMA) and phytohemagglutinin-A (PHA). RIPs for mRNAs associated with HuR and PABP (a quality control for the RIP-chip procedure) used earlier described methods and antibodies (Tenenbaum *et al*, 2000; Penalva *et al*, 2004; Keene *et al*, 2006). We conducted RIPs with PABP, a housekeeping RBP, as another indication for the biochemical specificity of the HuR IP, the primary focus of the study. Briefly, antibody-coated Protein-A Sepharose beads were incubated with cell lysates, thoroughly washed, and RNA was extracted from the pellets. For each time point, three biological replicates each of HuR, PABP, negative (IgG) RIP-chip pellets, and total cellular RNA (totals) samples were analyzed using oligo microarrays that interrogated 35K genes. To qualify for subsequent analysis and be treated as 'expressed', a probe had to be twofold above local background for all replicates in any of the IPs or the totals at any time point. For all probes expressed (n=14 789), t-scores for HuR-IP versus negative-IP were calculated using gene set enrichment analysis (GSEA) at each time point (Figure 1B, ST1). Visual inspection of the t-score distributions indicated two populations of mRNAs (Figures 1B and 2A): an enriched population representing HuR-associated mRNAs and a non-enriched population representing background mRNAs.

Gaussian mixture modeling (GMM), first devised in 1894 by Karl Pearson to discriminate genetic subpopulations of prawns based on carapace size (Pearson, 1894), was applied to identify and quantify biochemically enriched populations of mRNAs associated with HuR RNPs in a particular context of

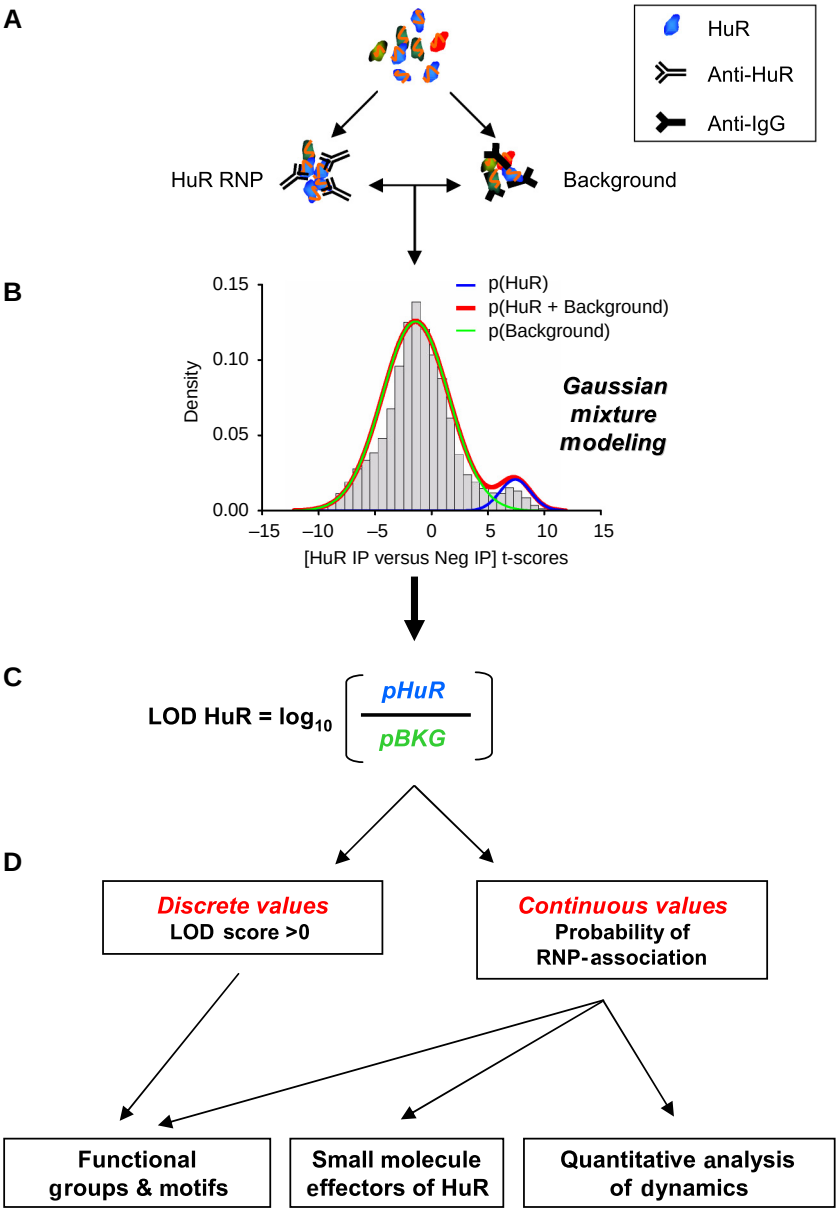

Figure 1 Overview of ribonomic analysis. (**A**) Isolation of HuR (blue) RNP complexes in parallel with IgG negative control, followed by extraction of mRNAs and hybridization to microarray (RIP chip). (**B**) GMM, of HuR IP versus negative IP t-scores for three biological replicates of RIP chip, to identify and quantify biochemically enriched populations mRNAs represented by probes. (**C**) LOD scores representing a condition-specific probability of HuR RNP association per probe. (**D**) Discrete approach, LOD HuR > 0, defines a subset of probes associated with HuR in a given biological condition. Continuous approach, LOD score values to compare HuR RNP mRNA dynamics across different biological conditions, with other data types or databases, and identify small molecule effectors of HuR. Both approaches identify common functional groups or motifs associated with HuR.

time or condition of treatment (Figure 1B) (Morris *et al*, 2008). Each component of the mixture model corresponded to a conditional probability of a t-score (the continuous variable) given class membership, 'target' or 'not target' (the discrete variable). Given the relative measure of enrichment, the t-score, we assigned class membership, 'target' or 'not target', based on the log of odds (LOD) ratio of the corresponding inferred mixtures. First, we treated RNP association as a discrete variable by modeling the continuous variable, the t-score, conditioned on the class membership to 'target' or 'not target'. Second, we treated RNP association as a continuous variable by providing a conditional probability for class membership given a t-score. Invariably, the model with the highest log-likelihood showed excellent fit to the data (Figure 2A, red curves) and discriminated the HuR-associated population (Figure 2A, blue curves) from background populations (Figure 2A, green curves) at all time points.

We generated values representing the probability of HuR association for each probe at each time point by calculating a LOD ratio comparing the weighted probability density function for the HuR-associated distribution to the sum of all background distributions based on a given probe's t-score

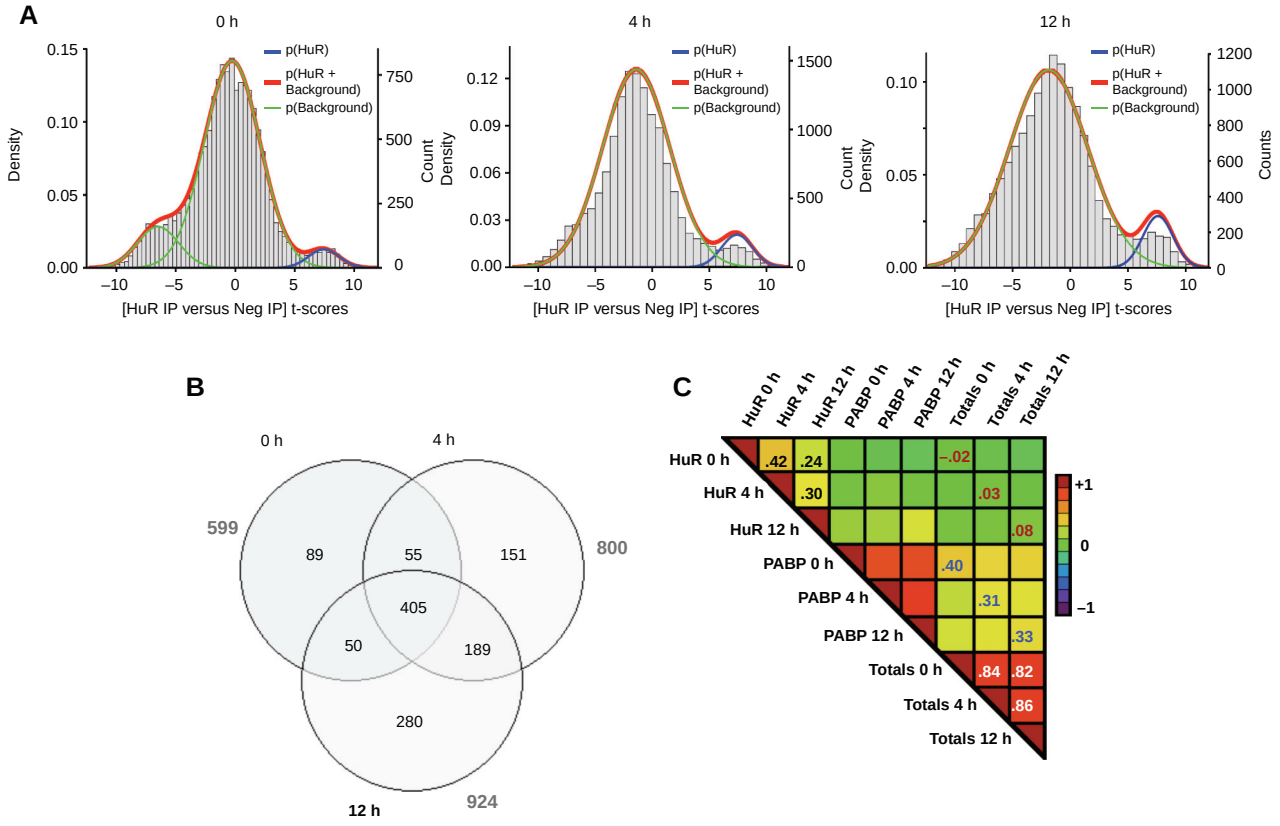

Figure 2 HuR RNP mRNA remodeling during Jurkat T-cell activation. (**A**) Distribution of HuR IP versus negative IP t-scores at 0, 4, and 12 h post-activation. HuR associated (blue curve), background (green curve), and sum of HuR associated and background (red curve) probability distributions are shown, as defined by GMM. (**B**) Venn diagram representing all probes (n=1219) that had an LOD HuR > 0 at any time point. (**C**) Upper triangular matrix of Spearman correlation coefficients for all pair-wise comparisons of LOD HuR and totals S_2N values for 0, 4, and 12 h post-activation.

(Figure 1C, ST1). The HuR LOD scores provide a continuous variable representing the condition-specific probability of HuR RNP association for each probe, allowing us to determine and to compare changes in the likelihood of HuR RNP association throughout the activation. Further, to gain insight into the similarities and differences of various layers of gene expression, we compared these LOD scores with other data types, such as transcriptomic data, and incorporated other datasets, such as other published RIP-chip experiments, into our analysis (Figure 1D).

Probes with HuR LOD scores greater than zero, thus having a higher likelihood of being within the HuR RNP-associated population in comparison with the background population, were considered to be a discrete population of mRNAs associated with HuR. Downstream analysis of the enrichment of an earlier reported and independently derived HuR-binding element (see HuR COVE motif below) suggested that the LOD > 0 cut-off was apt. Moreover, this threshold was substantiated in the ribonomic analysis of human Pum1 (Morris *et al*, 2008). Of the 14 789 probes expressed in the Jurkat cells, the number representing HuR targets increased from 599 (4.05%) to 800 (5.41%) to 924 (6.25%) probes at 0, 4, and 12 h post-activation, respectively (Figure 2B). Altogether, 1219 probes (the actual number of genes is lower, as multiple probes map to the same gene) were determined to be HuR targets for at least one of the time points. Of these, ~1/3 (405) were HuR targets at all time points. This shows the plasticity of HuR association during T-cell activation.

Complementarily to the comparisons of discrete values (target or not a target) above, we examined the quantitative differences in the mRNA content of HuR RNPs using continuous values representing condition-specific HuR RNP association for each probe (HuR LOD). As expected, for a given condition, there was very high correlation among the three independent biological replicates (average r=0.89, 0.92, and 0.93 for comparisons within 0, 4, and 12 h, respectively), showing the reproducibility of the RIP-chip method. Moreover, there were marked differences in the 0, 4, and 12 h HuR LOD scores as evidenced by the relatively low correlations between them (r=0.24–0.42), showing HuR-associated mRNA population dynamics (Figure 2C, black numbers). In comparison, the total mRNA levels were substantially more similar during the activation (r=0.82–0.86) (Figure 2C, white numbers), highlighting the dramatic remodeling of HuR RNPs during activation, as compared with the transcriptome. A more detailed analysis of HuR RNP dynamics is presented below.

We examined the relationships between HuR association, PABP association, and total mRNA expression level for probes considered as HuR targets at any time point. The steady-state PABP association resembled the transcriptome more than HuR

association (Figure 2C, blue numbers) at each time point. Notably, there was little to no correlation at 0, 4, or 12 h between the probability of HuR association and mRNA abundance (Figure 2C, red numbers), indicating that RIP chip successfully isolated specific subsets of mRNAs that were not quantitatively representative of total mRNA, consistent with our earlier studies (Tenenbaum *et al*, 2000; Morris *et al*, 2008).

Functional characteristics of HuR-associated mRNAs during activation

To identify the salient characteristics of the mRNA components of HuR RNPs at 0, 4, and 12 h post-activation, we analyzed the following (Figure 1D): (1) common sequence characteristics and motifs, (2) functional relationships among the proteins encoded by the HuR-associated mRNAs, and (3) interconnectivity between targets of microRNAs and RBPs, and the HuR-associated mRNAs.

Sequence characteristics and motifs enriched in HuR RNP mRNAs

As HuR typically binds elements in the 3′ UTR of transcripts, we searched for unique characteristics common among the 3′ UTR of HuR targets. Indeed, these transcripts have exceedingly long (1.54 kb, $P<0.0001$) and AU-rich (62.6%, $P<0.0001$) 3′ UTRs compared with randomly selected sets of UTRs (1.00 kb, 57.3%) (SF1). In addition, though HuR-associated mRNAs were enriched for the presence of computationally identified subclasses of AREs (Bakheet *et al*, 2001), there was no difference in propensity toward any subclass. Given that our results show that 3′ UTR length and AU content are good predictors of HuR association, and that HuR has no preference for any ARE subclass, combining global ARE RBP-target interaction data combined with computational approaches that use sequence and structural features may improve classification of AREs.

As noted above, an earlier study discovered a potential structural RNA motif for HuR binding by using covariance modeling (COVE) on 3′ UTR sequences of mRNAs identified from an HuR RIP-chip experiment in a different cell line and condition (Lopez de Silanes *et al*, 2004). We observed significant enrichment for all COVE-based metrics in the HuR-associated mRNAs at all time points (SF2). Surprisingly, the enrichment of COVE-based metrics for 3′ UTR sequences of HuR-associated mRNAs that had been randomized, while preserving dinucleotide frequencies, were not different from the enrichment for actual 3′ UTR sequences of HuR-associated mRNAs (SF2). This indicates that the HuR COVE motif does not identify a unique RNA structure, but rather strongly preferred sequence characteristics of 3′ UTRs that are capable of HuR binding.

Next, we used GSEA to determine how mRNAs that contain at least one HuR COVE motif in their 3′ UTR are distributed in the 0, 4, and 12 h lists ranked by HuR LOD scores. Enrichment profiles showed the usage of the COVE model for identifying elements in common to HuR RNP mRNAs (Figure 3), consistent with the results above. Moreover, the running enrichment score of the COVE motif peaked after LOD=0 for all time points (Figure 3), supporting the validity of the LOD>0 cut-off and indicating that it may be somewhat conservative.

Common functional groups enriched in HuR mRNA targets

As our experimental model is T-cell activation, we examined the HuR-associated mRNAs for encoded proteins with functions known to be critical in TCR engagement and local signaling, which involves adapter molecules, signal transduction, and cytoskeletal remodeling at the immunological synapse. HuR associated with 26 mRNAs critical to each of the aspects listed above (ST3). Moreover, all 26 mRNAs had at least one HuR COVE motif in its 3′ UTR. These data predict that HuR may help coordinate dynamic events directly downstream of TCR engagement after T-cell activation.

To determine if the proteins encoded by HuR-associated mRNAs were functionally related, we used Panther, InnateDB, and GSEA, which explore known relationships among a list of

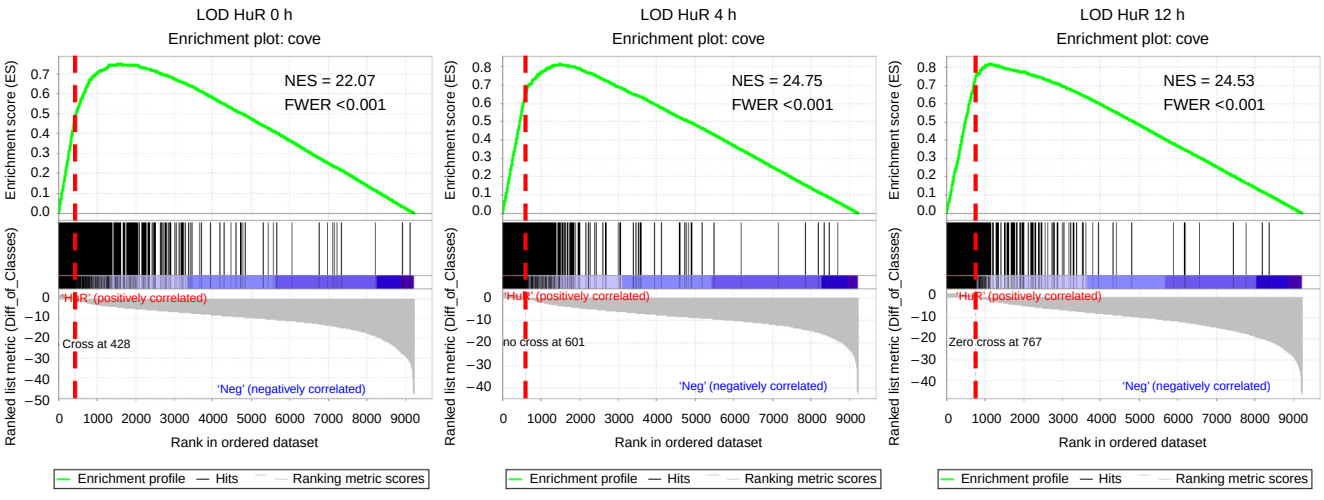

Figure 3 HuR RNP 3′ UTRs are enriched for HuR COVE motif. GSEA analysis of HuR LOD scores using HuR COVE motif gene set. Normalized enrichment scores (NES) and the FWER *P*-value are shown. LOD scores>0 are to the left of the vertical red line in the plots.

genes (Figure 1D). InnateDB and Panther analysis revealed significantly enriched pathways (Figure 4) vital to cellular function, for many of which regulation by HuR has been shown for individual members. These pathways include 'Wnt signaling' (Briata *et al*, 2003; Lopez de Silanes *et al*, 2003), 'metabotropic glutamate receptor group 1' (Tiruchinapalli *et al*, 2008), and 'p53 feedback loop 2' (Mazan-Mamczarz *et al*, 2003). GSEA on HuR LOD scores also identified pathways and perturbations in which HuR has known roles, such as aging (Wang *et al*, 2001), induced UVC stress (Wang *et al*, 2000b), and HCMV infection (Gealy *et al*, 2005) (for full list see ST2). Biological processes that HuR has been shown earlier to be involved in, such as the cell cycle (Wang *et al*, 2000a), and cell proliferation and differentiation (Atasoy *et al*, 1998), were also significantly enriched (Figure 4). 'Hedgehog signaling' and the 'circadian clock' represent novel pathways that may involve regulation by HuR. HuR-associated messages were also enriched for 'transcription', 'other transcription factors', 'mRNA processing', and 'other RBPs' (Figure 4); a defining characteristic of these categories is that they represent proteins that have important regulatory consequences for gene expression (Keene, 2007; Mansfield and Keene, 2009).

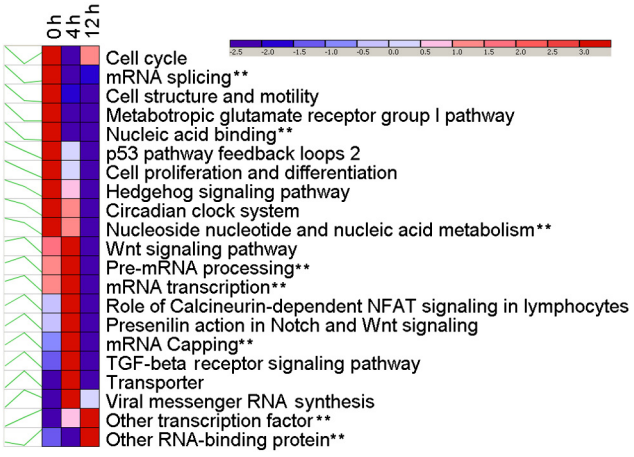

Figure 4 Coordination of HuR RNP-associated functional modules during T-cell activation. Analysis of HuR-associated mRNAs (LOD > 0) at each time point was conducted using Panther and InnateDB. Relative enrichment of functionally related groups (must have a Bonferroni corrected $P < 0.05$ for at least one time point) are represented as profiles and heatmap. **Functional groups that represent regulation of DNA and RNA.

Highly interconnected and combinatorial nature of HuR RNPs and posttranscriptional modules

We next explored mutual relationships between HuR RNPs and the ribonome, specifically focusing on regulatory RBPs and microRNAs. We asked the following questions: (1) Is there a bias for mRNAs of RBPs among the population of mRNAs associated with HuR RNPs, implicating HuR as a regulator of PTRFs? (2) Is the population of mRNAs associated with HuR enriched for known targets of ARE-RBPs and predicted targets of microRNAs, indicating that these mRNAs may be subject to combinatorial regulation?

First, we examined the hypothesis that HuR functions as a regulator of regulators in Jurkat cells, specifically of the group of adaptive mRNA subset-specific regulatory RBPs (Mesarovic *et al*, 2004; Penalva *et al*, 2004; Keene, 2007; Pullmann *et al*, 2007). We used a convenient catalog of RBPs that were compiled by Silver and co-workers identifying RBPs based on the presence of known RNA-binding domains, primarily RRM (RNA recognition motif) and hnRNP K homology domains (McKee *et al*, 2005). GSEA of HuR LOD scores showed that mRNAs encoding these RBPs were significantly enriched in HuR RNPs at all time points (Table I, ST4). Further, more than one half of the mRNAs encoding RBPs that associate with HuR were unique to at least one time point. The potential to regulate and coordinate mRNAs of regulatory RBPs indicates that HuR has a substantial role in the homeostasis and modulation of posttranscriptional regulatory networks (Mansfield and Keene, 2009).

The potential influence of other ARE-RBPs on HuR-associated mRNAs was assessed by creating gene sets for targets of *TTP* in activated mouse macrophage cells (RAW264.7) (Stoecklin *et al*, 2008), *TIAR* (Kim *et al*, 2007), and HuR (Lopez de Silanes *et al*, 2004) in human colon carcinoma cells (RKO). As HuR, *TTP*, and *TIAR* are all ARE-RBPs, and, therefore, putatively use similar *cis*-regulatory elements, we expected significant enrichment of lists ranked by HuR LOD scores. This was the case for RKO HuR RNP mRNAs (Table I,

Table I Enrichment of ribonomic gene sets in HuR RNP

Gene Sets Anlayzed	LOD HuR 0hr		LOD HuR 4hr		LOD HuR 12hr	
ENRICHED	NES	FDR	NES	FDR	NES	FDR
Regulatory RBPs	3.03	0.0002	3.11	0	2.83	0
TTP RNP (Activated RAW)	2.53	0.0006	2.64	0	2.89	0
HuR RNP (RKO)	1.62	0.0550	1.54	0.0809	2.03	0.0075
DEPLETED	NES	FDR	NES	FDR	NES	FDR
TIAR RNP (RKO)	-2.29	0.0015	-1.54	0.0657	-2.00	0.0099

GSEA analysis was conducted on LOD HuR scores for each time point using a gene set representing all regulatory RNA-binding proteins and experimentally derived RBP target gene sets. Normalized enrichment scores (NES) and the false discovery rate (FDR) *q*-value per gene set are shown. Red represents enriched, blue represents depleted.

ST5), which were significantly enriched (NES=2.03, false discovery rate (FDR)=0.0075) in the 12-h HuR RNPs and showed strong, but not statistically significant, enrichment (NES=1.62 and 1.54, FDR=0.0550 and 0.0809) in the 0 and 4 h HuR RNPs (Table I). As anticipated, *TTP* targets were significantly enriched (NES=2.53–2.89, FDR=0–0.0006) in the Jurkat HuR RNPs, suggesting that *TTP* RNPs and HuR RNPs are likely to contain many of the same mRNA species, and that *TTP* and HuR may in some cases co-occur on the same individual transcript. In contrast, the significant depletion (NES=−1.54 to −2.29, FDR=0.0015 to 0.0657) of *TIAR* targets (Table I) was consistent with the C-rich motif identified in *TIAR* target mRNAs, rather than AREs as initially believed (Gueydan *et al*, 1999).

A potential caveat to this comparative analysis was that each experiment was performed under different conditions and in different cell types, thus these observations could be explained by variations in condition-specific mRNA–RBP association. However, the consistency and strength of the enrichment for RKO HuR RNP mRNAs indicated that condition-specific association, although evident, did not confound interpretation of these RNP enrichment results. This indicates that cell-type and condition-specific differences in association do not explain the significant depletion of the *TIAR*-associated mRNAs, as the *TIAR* RIP-chip experiments were also performed using RKO cells. Thus, the dichotomy between global *TIAR* mRNA targets and the more similar HuR and *TTP* mRNA targets provides insight into the organization of posttranscriptional regulatory networks.

In addition to the analysis of RBP targets, we used gene sets corresponding to predicted targets of microRNAs (from MSigDb, http://www.broad.mit.edu/gsea/msigdb/) to obtain a comprehensive evaluation of the potential targeting of microRNAs to mRNAs associated with HuR RNPs. At all three time points, over 90 different microRNA target gene sets (Figure 5, ST6) were significantly enriched in HuR RNPs. The enrichment of microRNA target gene sets is especially striking when compared with the number of enriched gene sets representing transcription factor targets or curated gene sets (representing signaling pathways or experimental perturbations). Importantly, the biased enrichment of microRNA target gene sets compared with other classes of gene sets in the HuR IP was not recapitulated in either the PABP IP or the transcriptome (data not shown). Therefore, these analyses show that both microRNAs and regulatory RBPs have a high potential for combinatorial regulation of HuR RNP mRNAs, suggesting that the population of HuR-associated mRNAs represents a class of highly regulated transcripts.

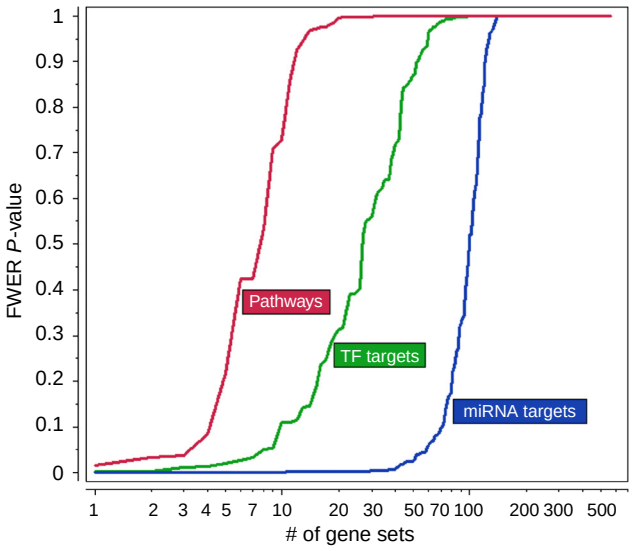

Figure 5 HuR RNPs are enriched for predicted targets of microRNAs. GSEA analysis was conducted on LOD HuR scores for each time point using the following three classes of gene sets for pathways, transcription factor targets (TF), and predicted microRNA (miRNA) target. Positively enriched gene sets were rank ordered and plotted by FWER *P*-values. Only results for 4 h are shown; 0 and 12 h results are similar.

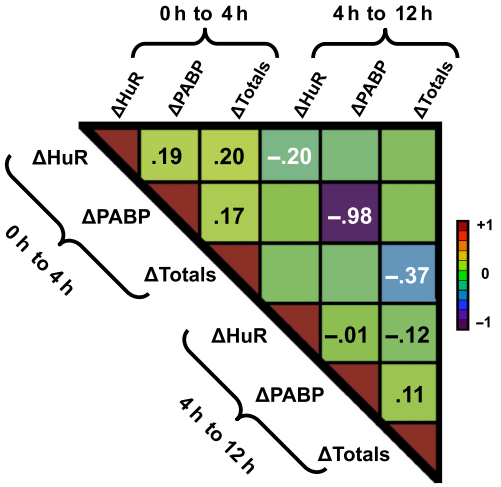

Figure 6 Gene expression dynamics show unique changes in mRNA subpopulations. Upper triangular matrix of Spearman correlation coefficients for all pair-wise comparisons of ΔLOD HuR, ΔLOD PABP, and totals t-scores for 0 to 4 h and 4 to 12 h dynamics.

RNP dynamics during activation

As the RNP LOD scores are condition specific, we calculated the difference between 0 and 4 h and 4 and 12 h for both HuR and PABP LOD scores to generate values representing changes in RNP association of these mRNAs. To assess changes in total mRNA, we generated t-scores comparing 0 to 4 h and 4 to 12 h time points. We excluded probes that had a low probability of being associated with HuR (LOD < 0 at all time points), as they would confound interpretation of changes across conditions.

Functional characteristics of ribonomic and transcriptomic dynamics during activation

We examined the similarity between HuR RNP, PABP RNP, and transcriptomic dynamics for 0 to 4 h (early) or 4 to 12 h (late) activation intervals. As expected, these values did not show strong correlations for early or late changes (r=−0.12–0.20) (Figure 6, black numbers), showing that each sample had unique overall gene expression dynamics. Importantly, the changes in HuR association were unique and were not explained by changes in mRNA abundance. Combined with

the earlier observation of cell-type and condition-specific differences in HuR association, we found no evidence that potential adventitious re-association (Mili and Steitz, 2004) was a concern in these data. As noted earlier (Keene *et al*, 2006), published criticisms (Ule *et al*, 2005) directed at this RIP-chip procedure were inappropriately applied by exploiting results from a different method that showed re-association of an HuR target from one cell to another in a sonicated extract (Mili and Steitz, 2004). Indeed, RIP chip has been used effectively by many laboratories without cross-linking, reviewed in Morris *et al* (2009). Within each data type, particularly PABP, there were reciprocal patterns of mRNA dynamics between early and late intervals (Figure 6, white circles). This may suggest a recovery from the activation and that increased temporal resolution would be informative. Although intriguing, the dynamics and the contrast of PABP-association profiles with the mRNA abundance profiles are outside the scope of this study.

Next, we identified common functional groups exhibiting HuR-association profiles that depending on condition, are either very similar to or very different from the transcriptomic profiles using rank-ordered pair-wise correlation profiles from all time points. We found that 'translation factors' were significantly enriched for negative correlation (ST7). Therefore, mRNAs encoding translation factors had HuR-association profiles that were the opposite of their transcriptomic profiles across the T-cell activation interval.

We made the analogous comparison between HuR-association profiles and PABP-association profiles. We observed two gene sets that were significantly enriched (ST7) and positively correlated, which was interesting, as both of these RBPs have been shown to be positive regulators of translation. One gene set represented transcripts that were up-regulated by the NF-kappa B transcription factor, a molecule critical to T-cell activation. The other gene set represented transcripts that were up-regulated at 4 h after PMA treatment and that discriminate PMA from other stress agents, as would be expected. This gene set was also enriched when examining early HuR RNP dynamics.

Functional characteristics of HuR RNP state dynamics during activation

Next, we identified functionally related mRNAs that exhibited common HuR RNP dynamics. GSEA analysis of HuR RNP dynamics was carried out for early changes (0 to 4 h) and late changes (4 to 12 h). For the early dynamics, the only significantly enriched gene set was the PMA-induced gene set, exhibiting increased HuR association from 0 to 4 h (ST7). For late dynamics, two gene sets were significantly enriched (ST7): (1) genes enriched in mouse neural stem cells compared with differentiated brain and bone marrow cells, which decreased in HuR association from 4 to 12 h and (2) genes with *LEF1* promoter elements, which showed increased HuR association from 4 to 12 h. Interestingly, HuR LOD scores for *LEF1* went from −0.29 at 0 h, to 1.37 at 4 h, to 1.13 at 12 h and the HuR promoter contains a predicted *LEF1*-binding site. The latter result raised the fascinating possibility of a translationally and transcriptionally coupled regulatory loop between HuR and *LEF1*.

Identification and validation of small molecule effectors of HuR

We hypothesized that HuR RNP dynamics could serve as a quantitative phenotype to explore the link between HuR and the physiological state of these cells. To test this possibility, we used the Connectivity Map (Lamb *et al*, 2006) (CMAP) to identify small molecules that could potentially modify functional states of HuR (Figure 1D). The CMAP is a tool that begins with a biological state of interest, specifically an *a priori* defined gene expression signature, and scans a database of perturbagen-induced transcriptomic profiles to connect the query signatures with small molecules based on correlation of gene expression dynamics. We used the 50 most dynamic mRNAs, those showing the greatest increase in HuR association and greatest decrease in HuR association, as a quantitative phenotype of HuR RNP mRNA dynamics to be compared with the CMAP profiles. The small molecule candidates that were identified for both early and late HuR RNP dynamics (Table II) may either mimic HuR functionality or act through HuR by yet to be determined mechanisms; using the 100 most dynamic mRNAs yielded very similar results (data not shown).

Many of the candidate HuR effectors fell into drug classes that have overlapping mechanisms of action, including PI3K, COX, HDAC, and Hsp90 inhibitors. HDAC inhibitors, which exert global effects on gene expression through chromatin remodeling, showed significant negative correlation with both early and late HuR-RNP dynamics. A negative correlation indicates that when the small molecule was tested in the set of cell lines used to prepare the CMAP, it induced changes in mRNA levels that were in the opposite direction of our observed changes in HuR association. Trichostatin A (TSA), a reversible HDAC inhibitor, has been shown to induce cell cycle arrest in Jurkat cells (Blagosklonny *et al*, 2002). Importantly, the identification of TSA represents an independent validation of our approach, as it has been shown to affect mRNA stability by decreasing the amount of cytoplasmic HuR in MCF7 (Pryzbylkowski *et al*, 2007) and RKO cells (Wang *et al*, 2004), breast and colon cancer lines, respectively, without affecting the total amount of HuR in the cell.

To further validate the outcomes of the CMAP analysis, we extensively examined a novel candidate from our list, resveratrol. First, we examined the effects of pretreatment with resveratrol on the subcellular distribution of HuR 0, 4, and 12 h post-activation. Regardless of pretreatment with resveratrol, overall levels of HuR protein did not change during the activation (data not shown). However, pretreatment with resveratrol resulted in an accumulation of endoplasmic reticulum/outer nuclear envelope (ER/ONE)-localized HuR and a concomitant depletion of nuclear-localized HuR 12 h post-activation (Figure 7). Thus, resveratrol pretreatment modulates the subcellular distribution of HuR during T-cell activation.

Next, we tested if resveratrol could have effects on posttranscriptional gene expression. We designed luciferase reporter constructs containing regions of the 3′ UTR from several of the top 50 most dynamic mRNAs that were used in the CMAP analysis (TNF-α, CSF2, ANP32A, and NAB2). Activation of the Jurkat cells induced a twofold or greater increase in expression (Figure 8A) for three of the four reporters (TNF-α, CSF2, and ANP32A). Pretreatment with resveratrol resulted in an ∼20–

Table II Candidate small molecule HuR effectors derived using CMAP

ΔHuR-RNP LOD scores		*0hr to 4hr*		*4hr to 12hr*	
Small Molecule	*Mechanism*	*ES*	*p-val*	*ES*	*p-val*
Acetylsalicylic acid	COX inhibitor	-0.709	**0.0492**	0	1
Sirolimus	mTOR Inhibitor	-0.574	**0.0014**	-0.417	**0.0463**
17-AAG	Hsp90 Inhibitor	-0.557	**0.0001**	0.301	0.0594
Resveratrol	COX Inhibitor	-0.511	0.1007	-0.562	**0.0495**
LY-294002	PI3K Inhibitor	-0.446	**0.0015**	0.33	**0.0374**
Deferoxamine	Iron Chelator	-0.415	0.5649	0.817	**0.0133**
Valproic acid	HDAC Inhibitor	-0.414	**0.0021**	0.301	0.0617
Wortmannin	PI3K Inhibitor	-0.353	0.2172	0.49	**0.0277**
Trichostatin A[a]	HDAC Inhibitor	-0.315	0.1549	0.747	**0**
Monorden	Hsp90 Inhibitor	-0.189	0.802	0.451	**0.0237**
Rofecoxib	COX Inhibitor	0	1	-0.552	**0.0299**
Vorinostat	HDAC Inhibitor	0	1	0.943	**0.0063**
Geldanamycin	Hsp90 Inhibitor	0.326	0.4547	0.728	**0.0008**
Raloxifene	SERM/Estrogen Inhibitor	0.547	0.2355	0.753	**0.0309**
Ikarugamycin	Endocytosis Inhibitor	0.779	**0.0221**	0.684	0.0635

Sign of enrichment scores (ES) represents whether changes in HuR association across the time course were either positively or negatively correlated with transcriptomic changes. Significant *P*-values (<0.05) listed in red.
[a]Known effector of HuR. Common classes of compounds are highlighted, Hsp90 inhibitors (blue), HDAC inhibitors (yellow), PI3K inhibitors (orange), and COX inhibitors (green).

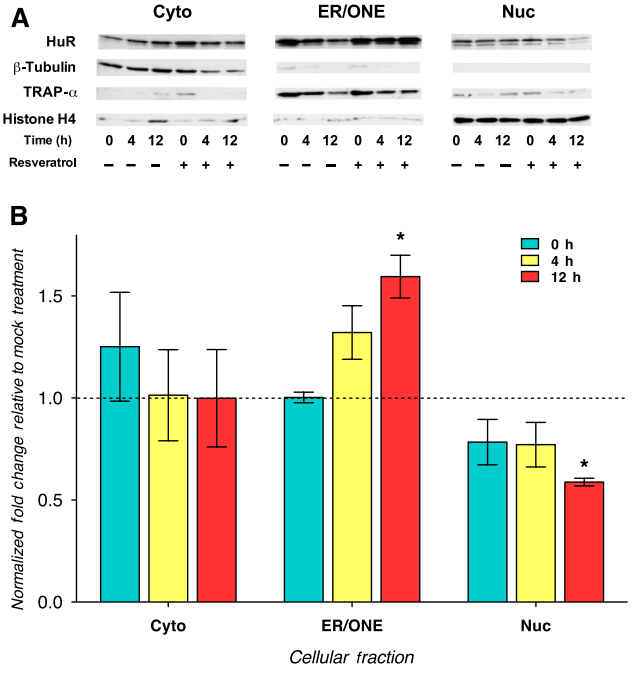

Figure 7 Resveratrol affects subcellular localization of HuR during activation. (**A**) Representative immunoblot of subcellular localization of HuR protein 0, 4, and 12 h post-activation of Jurkat cells using PMA and PHA with or without resveratrol pretreatment. Proteins were analyzed by immunoblot using anti-HuR, anti-β-tubulin as a cytosolic (Cyto) marker, anti-TRAP-α as an ER/ONE marker, and anti-histone h4 as a nuclear (Nuc) marker. Fourfold more Cyto and ER/ONE fraction extract was loaded compared with Nuc fraction extract. (**B**) Quantification of relative fold change in HuR after resveratrol pretreatment. HuR levels were normalized to the appropriate loading control for each fraction. Normalized HuR levels for resveratrol pretreated samples were compared with mock pretreated samples. The means and standard error of the means (s.e.m.) are represented from three independent experiments. Paired *t*-testes were used to calculate *P*-values (*$P<0.05$).

30% decrease in TNF-α, CSF2, and ANP32A reporter expression only in activated cells (Figure 8A). This suggests that resveratrol suppresses activation-induced increases in gene expression through one or more posttranscriptional mechanisms. However, resveratrol pretreatment did not suppress reporter expression of activated Jurkat cells when co-transfected with HuR (Figure 8B). Therefore, these data indicate that HuR can partially rescue resveratrol-mediated posttranscriptional suppression of reporter expression in activated Jurkat cells, suggesting that HuR has a role in the effects of resveratrol on these cells.

In summary, the results of our analysis of HuR RNP dynamics using the CMAP led to the following conclusions: (1) quantification of HuR RNP dynamics from ribonomic profiling-identified effectors capable of modulating HuR; (2) as we defined our biological state of interest based on HuR RNP dynamics rather than transcriptomic signature, this represents a novel application of the CMAP; and (3) small molecule drugs can have posttranscriptional consequences for cells that are largely unknown and uninvestigated.

Discussion

GMM is one of the many diverse approaches to analyze RIP-chip data (Tenenbaum *et al*, 2000; Gerber *et al*, 2004; Lopez de Silanes *et al*, 2004; Townley-Tilson *et al*, 2006; Stoecklin *et al*, 2008). The advantage of probabilistic mixture modeling, such as GMM, is the full specification of the distribution generating the data. In our case, this results in the specification of a Gaussian distribution for each mixture and the probability of an mRNA belonging to each mixture. Using this model, we can discriminate HuR-associated mRNAs from background mRNAs, as well as generate condition-specific probabilities of association. This is especially useful for assessing condition-

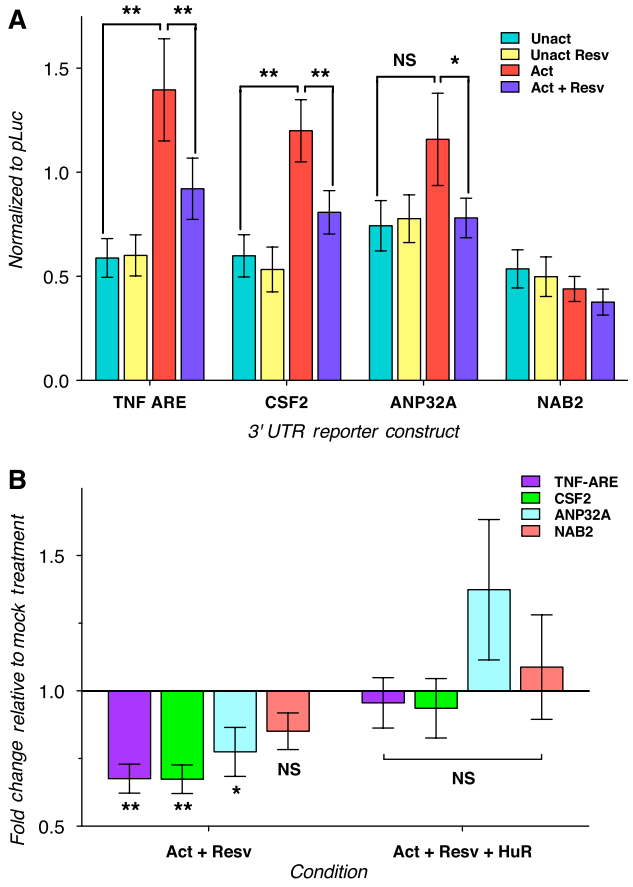

Figure 8 Activation-dependent effects of resveratrol and HuR on 3′ UTR luciferase reporters. (**A**) Firefly to renilla ratio of each reporter normalized to the control 3′ UTR reporter, pLuc, for each condition. Activation significantly increases reporter expression through specific sequences. Furthermore, resveratrol significantly blunts this increase. (**B**) The fold change of the normalized firefly to renilla ratio for the indicated condition (activation + resveratrol or activation + resveratrol + HuR) compared with the normalized firefly to renilla ratio for its matched mock-treated control. As shown in (A) resveratrol inhibits activation-mediated increases in reporter expression; however, (B) shows that HuR overexpression antagonizes resveratrol-dependent inhibition. The means and standard error of the means (s.e.m.) are represented from 7 to 10 independent experiments. Paired *t*-tests were used to calculate *P*-values (*$P<0.05$, **$P<0.01$).

specific differences in the likelihood of RNP association for all mRNAs detected. Such a probabilistic framework is particularly appealing given the stochasticity in gene expression among individual cells and the consequent heterogeneity within a population of cells implicit in most biological experiments (Newman *et al*, 2006; Wilkinson, 2009).

Our results show dramatic remodeling of HuR RNPs during T-cell activation, especially compared with transcriptomic expression dynamics (Figure 2). RNP remodeling of functionally related mRNAs was observed earlier with HuB, another member of the ELAV/Hu family, during retinoic acid-induced neuronal differentiation of P19 embryonic carcinoma cells (Tenenbaum *et al*, 2000). In this study, we uncovered temporally coordinated changes in populations of HuR-associated mRNAs whose encoded proteins are functionally related and necessary for T-cell activation (ST3) and Wnt signaling (Figure 4), consistent with the PTRO model.

HuR-associated functional modules

Our data predict that HuR has a role in coordinating post-transcriptional events imminent to TCR signaling (ST3). Signaling elicited by TCR engagement results in the formation of supramolecular activation clusters at the immunological synapse and in T-cell selection. Our prediction was validated by the finding of TCR signaling defects-obstructed activation-driven positive selection in a thymus-specific knockout of HuR in mouse (Papadaki *et al*, 2009). Further corroborating the importance of HuR in T-cell activation, chemical inhibition of HuR–mRNA interaction has been shown to inhibit nucleo-cytoplasmic redistribution of HuR and to block T-cell activation (Meisner *et al*, 2007).

Our data suggest that HuR may regulate many members of the Wnt pathway during T-cell activation, consistent with the earlier studies showing regulation of the β-catenin mRNA by HuR (Lopez de Silanes *et al*, 2003; Thiele *et al*, 2006). Moreover, Wnt signaling induces the stabilization of the PITX2 transcription factor and downstream target mRNAs through an increase in association with HuR (Briata *et al*, 2003). Similarly, we found another transcription factor involved in Wnt signaling, LEF1, and its downstream targets increase in HuR association from 4 to 12 h (ST7). The Wnt signaling pathway is a key regulator of T-cell development in the thymus (Staal and Clevers, 2003); however, its role in T-cell activation, to our knowledge, has not been examined. Therefore, the interdependence between HuR and the Wnt pathway during T-cell activation warrants further investigation in cellular and animal models.

HuR-association dynamics

Posttranslational modifications and changes in sub-cellular concentrations of HuR may be potential mechanisms driving our reported population dynamics. Thus far, each posttranslational modification identified has been accompanied by changes in the subcellular localization of HuR, as well as functional implications for mRNA stability and/or translation of one or more target mRNAs (Li *et al*, 2002; Abdelmohsen *et al*, 2007; Doller *et al*, 2007; Kim *et al*, 2008). However, a recent study showed differences in association without a difference in subcellular localization (Silanes *et al*, 2009). PKC-α-mediated phosphorylation of HuR is particularly significant to our study, as PMA is a potent stimulator of PKC activity. Furthermore, one of the two sites critical for phosphorylation by PKC-α is in the second RRM of HuR and may affect RNA binding by HuR. In addition, Chk2-induced phosphorylation of HuR results in differential association and expression of an mRNA target, SIRT1 (Abdelmohsen *et al*, 2007). Therefore, we hypothesize that posttranslational modification of HuR is a mechanism that contributes to HuR-association dynamics during T-cell activation.

Dynamics in HuR association could also be influenced by the abundance or availability of target mRNAs. Owing to the lack of correlation between HuR association and mRNA abundance, it is unlikely that differences in the amount of target mRNA is the sole determinant of HuR mRNA population dynamics (Figures 2 and 6). Conversely, we observed a high potential for HuR targets to be combinatorially regulated by other PTRFs, for example microRNAs and TTP (Figure 5;

Table I). Therefore, competition by other PTRFs may affect the availability of target mRNAs for HuR and may be a mechanism influencing the observed HuR-association dynamics.

HuR and small molecules

On the basis of HuR RNP dynamics, we identified classes of small molecule candidates that can modulate HuR functionality using the CMAP (Table II). We show for the first time that RNP dynamics can be used as a quantitative phenotype to systematically identify compounds that exert posttranscriptional effects and modulate the corresponding RBP, in this case, HuR (Figures 7 and 8).

Hsp90 inhibitors are a class of small molecule drugs for which multiple candidate compounds were identified, specifically geldanamycin, monorden, and 17-AAG. It was shown earlier that during LPS activation of macrophages, treatment with geldanamycin resulted in decreased production of inhibitory cytokines (Wax *et al*, 2003) by negatively affecting stability and translation of cytokine mRNAs, including those known to be regulated by HuR.

We found that resveratrol, a COX inhibitor that exhibits anti-inflammatory and chemopreventive effects, modulates the subcellular localization of HuR during activation (Figure 7). In addition, our data show that resveratrol can suppress activation-induced gene expression (Figure 8). Similarly, an earlier study showed that resveratrol suppresses TNF-dependent activation of transcription factors in PMA-treated Jurkat cells (Manna *et al*, 2000). However, our results reveal a posttranscriptional component to effects of resveratrol. Interestingly, as we show resveratrol suppresses activation-induced increase in TNF reporter expression, this could be a mechanism working upstream of TNF-dependent activation of transcription factors during T-cell activation. Furthermore, we observed that HuR antagonized the resveratrol-mediated effects on gene expression. Therefore, we can systematically identify compounds that modulate RBP function, and have posttranscriptional consequences for gene expression, and whose effects can be rescued by the RBP being examined.

In addition, resveratrol, which is found in red wine, exhibits anti-aging properties putatively through activation of sirtuin-1 (SIRT1), a known HuR target. Indeed, overexpression of HuR in senescent cells restores a 'younger' phenotype (Wang *et al*, 2001). Studies using models of senescence showed correlated decreases in both HuR levels and the stability of target mRNAs involved in aging, including SIRT1 (Abdelmohsen *et al*, 2007). Not only did we find SIRT1 as an HuR target (ST1), we also found that genes reported to have reduced expression in the brains of human beings after the age of 40 (Lu *et al*, 2004) were significantly enriched as HuR targets (ST2). Given our results, earlier studies, and the promise of resveratrol as a compound to prevent aging, cancer, and inflammation, it will be critical to understand the posttranscriptional effects of resveratrol and the role of HuR and other PTRFs in these effects.

Combinatorial Interdependence and the PTRO model

Our data establish that HuR-associated mRNAs are significantly enriched for predicted targets of over 90 microRNAs and TTP targets (Table I, Figure 5, ST6). As HuR can promote mRNA stability and translation, the presence of microRNAs and RBPs, such as TTP, which promote mRNA degradation and/or translational repression, in HuR RNPs suggests competition with HuR, resulting in opposing functional outcomes. Indeed, competition between HuR and TTP has been shown for individual mRNAs, specifically IL-3 (Ming *et al*, 2001) and TNF-α (Katsanou *et al*, 2005). In addition, HuR was shown to be essential for the relief of microRNA-mediated repression of the CAT-1 mRNA in stressed cells (Bhattacharyya *et al*, 2006). Interestingly, miR-181 targets are one of the most enriched microRNA target gene sets for HuR association and the most depleted for PABP association. Similar to HuR, miR-181a has been shown to modulate TCR signaling and T-cell selection (Li *et al*, 2007). Our data suggest that the targeting of these functionally antagonistic mechanisms is more widespread than currently believed, yet specific to subsets of transcripts. This is consistent with the PTRO model that predicts combinatorial interactions by RBPs and microRNAs that either compete or cooperate to determine the final functional outcomes that are shared by a subset of functionally related mRNAs (Keene and Lager, 2005; Keene, 2007).

Regulation of gene expression involves two linked, but very different processes: control and coordination. Although posttranscriptional 'control' indicates a distinct outcome for a single transcript directed by one or more *trans*-factors, 'coordination' involves orchestration across multiple control functions, temporally and spatially, of multiple transcripts to achieve harmonization. It is a challenge to determine mechanisms of control across entire sets of transcripts when most molecular interactions are combinatorial (Table I; Figure 5) and yet to be discovered. Therefore, these interactions need to be understood on a global basis before one can understand how gene expression systems can be both balanced and agile in response to biological signals. Probabilistic modeling of mRNA states, as described in this paper, will help provide a better understanding of mRNA coordination as well as control functions. More importantly, global patterns of control functions could be used to infer the coordination logic of the proposed PTRO model.

Materials and methods

Cell culture

Jurkat cells were cultured in RPMI 1640 supplemented with 10% FBS (GIBCO). For activation, cells were treated with 50 ng/ml PMA and 2 μg/ml PHA (Calbiochem, San Diego, CA, USA). Cells were pretreated with 50 μM resveratrol for 2 h and then subject treated with PMA/PHA.

Immunoprecipitation assays and RNA isolation

Lysates were prepared from samples collected at 0, 4, and 12 h post-activation as described, with the addition of 10% glycerol to the polysome lysis buffer (PLB) and resuspension of harvested cells in PLB. RIP of endogenous HuR and PABP RNP complexes were used to assess association of endogenous target mRNAs. Assays were performed as described (Tenenbaum *et al*, 2000; Penalva *et al*, 2004). RIPs used 100 μl pre-swollen and packed Protein-A Sepharose beads (Sigma) loaded with 30 μg of anti-HuR (3A2), anti-PABPC1 serum and anti-PABPC4 serum (sera generated in Penalva *et al*, 2004), and mouse IgG1. Antibody loaded beads were incubated with 3 mg cell lysate for 4 h at 4 °C, washed four times with ice-cold NT2 buffer

(50 mM Tris pH 7.4/150 mM NaCl/1 mM MgCl2/0.05% Nonidet P-40) followed by three washes with ice-cold NT2 supplemented with 1 M Urea. Extraction of associated RNA was performed as described, and total RNA was isolated using the Trizol (Invitrogen).

Microarray analysis

Arrays were printed at the Duke Array Facility using the Genomics Solutions OmniGrid300 Arrayer and contained Human Operon v3.0.2 oligo set (Oligo Source) consisting of ~35k unique 70-mers. RNA quality was checked using an Agilent2100 bioanalyzer (Agilent technologies) for total RNA samples only. For all arrays, RNA was assayed using direct labeling of experimental samples (Cy 3) and Stratagene Universal Human Reference RNA (Cy 5). Array data were submitted to the GEO, GSE11989. All arrays were subject to loess normalization within each array and scale normalization across arrays using the Array Magic (Buness *et al*, 2005). Replicate probes were collapsed to the median value. To be considered for subsequent analysis, probes had to be two times greater than the local background in all biological replicates for any of the RIPs or the totals at any time point.

Determining RNP association

GSEA was used to calculate t-scores comparing the RNP IP to matching the IgG IP. GMM was performed multiple times on the t-score distributions to estimate the mean, standard deviation, and weight of each component using the Mixtools package in R (Young *et al*, 2007). The number of components was determined by visual inspection. As this implementation of GMM used expectation maximization, which is prone to convergence on local optimum, multiple runs of GMM were conducted that initialized at different points. The parameters from the model with the highest likelihood were used to create LOD scores of HuR association by comparing the weighted probability density functions of the HuR-associated versus the background distribution or in the case of multiple 'non-enriched' populations the sum of the background distributions.

Ribonomic-transcriptomic comparisons

For values representing mRNA abundance, we calculated a signal-to-noise (S_2N) ratio (to account for variance across replicates) for the three biological replicates per time point. The Spearman correlation coefficient between HuR-association, PABP-association, and mRNA abundance profiles across all time points were calculated per probe. GSEA was used to calculate t-scores per probe representing differential expression between 0 and 4 h and 4 and 12 h. Upper triangular matrix color maps were made using JMP 7.0 (SAS).

Sequence characteristics

We used a local pipeline to retrieve high quality 3′ UTR sequence for all transcripts expressed (Majoros and Ohler, 2007). The AU content and length of each UTR was calculated. We mapped the ARED 3.0 database to refseqs to determine which transcript contained either class I or class II AREs. COVE-LS was used to search sequences using the HuR COVE model and the following statistics were calculated: at least one match, number of matches, maximum score, sum of all scores, and the average of scores. Significance of the enrichment of each HuR COVE model statistic was tested using random sampling. Null distributions were created for each characteristic listed above by calculating the average of randomly chosen sets from total expressed population (10 000 random sets, with the same # of UTRs as HuR-associated set) and compared with the average value for the HuR-associated mRNAs to determine statistical significance. Null distribution for assessing the contribution of secondary structure to HuR COVE model statistics was created by calculating the average of randomly generated dinucleotide shuffled sequence from 3′ UTRs associated with HuR (1000 sets) and compared with the average value calculated above for the actual 3′ UTR sequence of HuR-associated mRNAs to determine statistical significance.

Functional enrichment

GSEA (Subramanian *et al*, 2005), Panther (Mi *et al*, 2007), and InnateDB (Lynn *et al*, 2008) were used for enrichments. A gene set had an FDR q-value <0.05 or family-wise error rate (FWER) <0.1 to be considered significant for all GSEA analysis. For non-Gaussian data, the classic enrichment statistic was used. For Panther and InnateDB analysis, gene sets were required to have a Bonferroni corrected P-value <0.05.

Plasmids

The Firefly-UTR reporters used for this study were generated by cloning the UTR fragemts into the NotI and ApaI sites of pCDNA3-Luc. Fragments of the UTRs were created using the following primers:

TNF ARE-Fwd TCCAGATGTTTCCAGACTTC
TNF ARE-Rev TGAGCCAAGGCAGCTCCTAC
CSF2-Fwd TGATACAGGCATGGCAGAAG
CSF2-Rev TACGGTAAAACATCTTGAATAAATATG
ANP32A-Fwd AGTGGAATAACCTATTTTGAAAAATTC
ANP32A-Rev CATTCTTTTTACAATACGACAAACAAA
NAB2-Fwd AGGGTTGGACTGGTGTCTTC
NAB2-Rev GCCATAAAATAAATTTTATTCCAAA

pRL, pCDNA3-HuR, and pCDNA3 were used in this study as well.

Transfections

Transfections were performed using Lipofectamine 2000 (Invitrogen) using the standard protocol. Briefly, 1.6 μg of total DNA was diluted in 100 μl of Opti-MEM I (GIBCO) and mixed with 4 μl of Lipofectamine 2000 diluted in 100 μl of Opti-MEM I and incubated at room temperature for 30 min. 1×10^6 Jurkats were plated in fresh media in 12-well plates. The re-plated cells were then immediately and mixed with the DNA/Lipofectamine 2000 complexes. The Luciferase reporter plasmids were transfected in equimolar amounts, 20 pmoles for each of the Firefly-UTR constructs and 10 pmoles for the Renilla construct. 0.5 μg of pCDNA3-HuR was co-transfected in indicated experiments and the remainder of the transfection mix was brought to 1.6 μg using the pCDNA3 vector.

Cell fractionation

Cells were collected, washed with PBS and then subject to an earlier described fractionation protocol (Atasoy *et al*, 1998). Cytoplasmic, ER/ONE and nuclear fraction control antibodies included anti-B–Tubulin (Harlan Sera-Lab), anti-TRAP-α (kindly provided by Chris Nicchitta), and Histone H4 (Abcam), respectively. Protein bands were quantified using GelEval (Frog Dance Software).

Luciferase assay

Luciferase assays were performed using the Dual-Luciferase Reporter Assay System (Promega). Transfected cells were pretreated with 50 nM Resveratrol for 2 h and then activated with 50 ng/ml PMA and 2 μg /ml PHA for 4 h. The cells were then collected and washed with PBS and then lysed with 100 μl of 1 × passive lysis buffer. For both cell fractionation and luciferase experiments, paired t-tests were performed in GraphPad Prism (GraphPad Software).

Supplementary information

Supplementary information is available at the *Molecular Systems Biology* website (www.nature.com/msb).

Acknowledgements

We thank Uwe Ohler and William Majoros for access to the 3′ UTR database, Sayan Mukherjee for valuable advice on statistical analyses, and Shelton Bradrick and Keene laboratory members for helpful comments regarding the manuscript.

Conflict of interest

JDK has a financial relationship with Ribonomics, Inc and MBL, Inc that holds licenses to technologies relevant to aspects of this study. The other co-authors have no known conflicts of interest.

References

Abdelmohsen K, Pullmann Jr R, Lal A, Kim HH, Galban S, Yang X, Blethrow JD, Walker M, Shubert J, Gillespie DA, Furneaux H, Gorospe M (2007) Phosphorylation of HuR by Chk2 regulates SIRT1 expression. *Mol Cell* **25:** 543–557

Atasoy U, Watson J, Patel D, Keene JD (1998) ELAV protein HuA (HuR) can redistribute between nucleus and cytoplasm and is upregulated during serum stimulation and T cell activation. *J Cell Sci* **111:** 3145–3156

Bakheet T, Frevel M, Williams BR, Greer W, Khabar KS (2001) ARED: human AU-rich element-containing mRNA database reveals an unexpectedly diverse functional repertoire of encoded proteins. *Nucleic Acids Res* **29:** 246–254

Bhattacharyya SN, Habermacher R, Martine U, Closs EI, Filipowicz W (2006) Relief of microRNA-mediated translational repression in human cells subjected to stress. *Cell* **125:** 1111–1124

Blagosklonny MV, Robey R, Sackett DL, Du L, Traganos F, Darzynkiewicz Z, Fojo T, Bates SE (2002) Histone deacetylase inhibitors all induce p21 but differentially cause tubulin acetylation, mitotic arrest, and cytotoxicity. *Mol Cancer Ther* **1:** 937–941

Brengues M, Teixeira D, Parker R (2005) Movement of eukaryotic mRNAs between polysomes and cytoplasmic processing bodies. *Science (New York, NY)* **310:** 486–489

Briata P, Ilengo C, Corte G, Moroni C, Rosenfeld MG, Chen CY, Gherzi R (2003) The Wnt/beta-catenin—>Pitx2 pathway controls the turnover of Pitx2 and other unstable mRNAs. *Mol Cell* **12:** 1201–1211

Buness A, Huber W, Steiner K, Sultmann H, Poustka A (2005) ArrayMagic: two-colour cDNA microarray quality control and preprocessing. *Bioinformatics* **21:** 554–556

Cheadle C, Fan J, Cho-Chung YS, Werner T, Ray J, Do L, Gorospe M, Becker KG (2005) Control of gene expression during T cell activation: alternate regulation of mRNA transcription and mRNA stability. *BMC Genomics* **6:** 75

Doller A, Huwiler A, Muller R, Radeke HH, Pfeilschifter J, Eberhardt W (2007) Protein kinase C alpha-dependent phosphorylation of the mRNA-stabilizing factor HuR: implications for posttranscriptional regulation of cyclooxygenase-2. *Mol Biol Cell* **18:** 2137–2148

Fan XC, Steitz JA (1998) Overexpression of HuR, a nuclear-cytoplasmic shuttling protein, increases the *in vivo* stability of ARE-containing mRNAs. *EMBO J* **17:** 3448–3460

Gealy C, Denson M, Humphreys C, McSharry B, Wilkinson G, Caswell R (2005) Posttranscriptional suppression of interleukin-6 production by human cytomegalovirus. *J Virol* **79:** 472–485

Gerber AP, Herschlag D, Brown PO (2004) Extensive association of functionally and cytotopically related mRNAs with puf family RNA-binding proteins in yeast. *PLoS Biol* **2:** e79

Gueydan C, Droogmans L, Chalon P, Huez G, Caput D, Kruys V (1999) Identification of TIAR as a protein binding to the translational regulatory AU-rich element of tumor necrosis factor alpha mRNA. *J Biol Chem* **274:** 2322–2326

Halbeisen RE, Galgano A, Scherrer T, Gerber AP (2008) Post-transcriptional gene regulation: from genome-wide studies to principles. *Cell Mol Life Sci* **65:** 798–813

Hogan DJ, Riordan DP, Gerber AP, Herschlag D, Brown PO (2008) Diverse RNA-binding proteins interact with functionally related sets of RNAs, suggesting an extensive regulatory system. *PLoS Biol* **6:** e255

Ip JY, Tong A, Pan Q, Topp JD, Blencowe BJ, Lynch KW (2007) Global analysis of alternative splicing during T-cell activation. *RNA (New York, NY)* **13:** 563–572

Jain RG, Andrews LG, McGowan KM, Pekala PH, Keene JD (1997) Ectopic expression of Hel-N1, an RNA-binding protein, increases glucose transporter (GLUT1) expression in 3T3-L1 adipocytes. *Mol Cell Biol* **17:** 954–962

Katsanou V, Papadaki O, Milatos S, Blackshear PJ, Anderson P, Kollias G, Kontoyiannis DL (2005) HuR as a negative posttranscriptional modulator in inflammation. *Mol Cell* **19:** 777–789

Keene JD (2001) Ribonucleoprotein infrastructure regulating the flow of genetic information between the genome and the proteome. *PNAS* **98:** 7018–7024

Keene JD (2007) RNA regulons: coordination of post-transcriptional events. *Nat Rev* **8:** 533–543

Keene JD, Komisarow JM, Friedersdorf MB (2006) RIP-Chip: the isolation and identification of mRNAs, microRNAs and protein components of ribonucleoprotein complexes from cell extracts. *Nat Protoc* **1:** 302–307

Keene JD, Lager PJ (2005) Post-transcriptional operons and regulons co-ordinating gene expression. *Chromosome Res* **13:** 327–337

Keene JD, Tenenbaum SA (2002) Eukaryotic mRNPs may represent posttranscriptional operons. *Mol Cell* **9:** 1161–1167

Kim HH, Abdelmohsen K, Lal A, Pullmann Jr R, Yang X, Galban S, Srikantan S, Martindale JL, Shokat KM, Gorospe M (2008) Nuclear HuR accumulation through phosphorylation by Cdk1. *Genes Dev* **22:** 1804–1815

Kim HS, Kuwano Y, Zhan M, Pullmann Jr R, Mazan-Mamczarz K, Li H, Kedersha N, Anderson P, Wilce MC, Gorospe M, Wilce JA (2007) Elucidation of a C-rich signature motif in target mRNAs of RNA-binding protein TIAR. *Mol Cell Biol* **27:** 6806–6817

Lam LT, Pickeral OK, Peng AC, Rosenwald A, Hurt EM, Giltnane JM, Averett LM, Zhao H, Davis RE, Sathyamoorthy M, Wahl LM, Harris ED, Mikovits JA, Monks AP, Hollingshead MG, Sausville EA, Staudt LM (2001) Genomic-scale measurement of mRNA turnover and the mechanisms of action of the anti-cancer drug flavopiridol. *Genome Biol* **2:** RESEARCH0041

Lamb J, Crawford ED, Peck D, Modell JW, Blat IC, Wrobel MJ, Lerner J, Brunet JP, Subramanian A, Ross KN, Reich M, Hieronymus H, Wei G, Armstrong SA, Haggarty SJ, Clemons PA, Wei R, Carr SA, Lander ES, Golub TR (2006) The Connectivity Map: using gene-expression signatures to connect small molecules, genes, and disease. *Science (New York, NY)* **313:** 1929–1935

Levine TD, Gao F, King PH, Andrews LG, Keene JD (1993) Hel-N1: an autoimmune RNA-binding protein with specificity for 3′ uridylate-rich untranslated regions of growth factor mRNAs. *Mol Cell Biol* **13:** 3494–3504

Li H, Park S, Kilburn B, Jelinek MA, Henschen-Edman A, Aswad DW, Stallcup MR, Laird-Offringa IA (2002) Lipopolysaccharide-induced methylation of HuR, an mRNA-stabilizing protein, by CARM1. Coactivator-associated arginine methyltransferase. *J Biol Chem* **277:** 44623–44630

Li QJ, Chau J, Ebert PJ, Sylvester G, Min H, Liu G, Braich R, Manoharan M, Soutschek J, Skare P, Klein LO, Davis MM, Chen CZ (2007) miR-181a is an intrinsic modulator of T cell sensitivity and selection. *Cell* **129:** 147–161

Lopez de Silanes I, Fan J, Yang X, Zonderman AB, Potapova O, Pizer ES, Gorospe M (2003) Role of the RNA-binding protein HuR in colon carcinogenesis. *Oncogene* **22:** 7146–7154

Lopez de Silanes I, Zhan M, Lal A, Yang X, Gorospe M (2004) Identification of a target RNA motif for RNA-binding protein HuR. *Proc Natl Acad Sci USA* **101:** 2987–2992

Lu T, Pan Y, Kao SY, Li C, Kohane I, Chan J, Yankner BA (2004) Gene regulation and DNA damage in the ageing human brain. *Nature* **429:** 883–891

Lynn DJ, Winsor GL, Chan C, Richard N, Laird MR, Barsky A, Gardy JL, Roche FM, Chan TH, Shah N, Lo R, Naseer M, Que J, Yau M, Acab M, Tulpan D, Whiteside MD, Chikatamarla A, Mah B, Munzner T *et al.* (2008) InnateDB: facilitating systems-level analyses of the mammalian innate immune response. *Mol Syst Biol* **4:** 218

Majoros WH, Ohler U (2007) Spatial preferences of microRNA targets in 3′ untranslated regions. *BMC Genomics* **8:** 152

Manna SK, Mukhopadhyay A, Aggarwal BB (2000) Resveratrol suppresses TNF-induced activation of nuclear transcription factors NF-kappa B, activator protein-1, and apoptosis: potential role of reactive oxygen intermediates and lipid peroxidation. *J Immunol* **164:** 6509–6519

Mansfield KD, Keene JD (2009) The Ribonome: A Dominant Force in Coordinating Gene Expression. *Biol Cell* **101:** 169–181

Mazan-Mamczarz K, Galban S, Lopez de Silanes I, Martindale JL, Atasoy U, Keene JD, Gorospe M (2003) RNA-binding protein HuR enhances p53 translation in response to ultraviolet light irradiation. *Proc Natl Acad Sci USA* **100:** 8354–8359

Mazan-Mamczarz K, Hagner PR, Corl S, Srikantan S, Wood WH, Becker KG, Gorospe M, Keene JD, Levenson AS, Gartenhaus RB (2008a) Post-transcriptional gene regulation by HuR promotes a more tumorigenic phenotype. *Oncogene* **27:** 6151–6163

Mazan-Mamczarz K, Hagner PR, Dai B, Wood WH, Zhang Y, Becker KG, Liu Z, Gartenhaus RB (2008b) Identification of transformation-related pathways in a breast epithelial cell model using a ribonomics approach. *Cancer Res* **68:** 7730–7735

McKee AE, Minet E, Stern C, Riahi S, Stiles CD, Silver PA (2005) A genome-wide *in situ* hybridization map of RNA-binding proteins reveals anatomically restricted expression in the developing mouse brain. *BMC Dev Biol* **5:** 14

Meisner NC, Hintersteiner M, Mueller K, Bauer R, Seifert JM, Naegeli HU, Ottl J, Oberer L, Guenat C, Moss S, Harrer N, Woisetschlaeger M, Buehler C, Uhl V, Auer M (2007) Identification and mechanistic characterization of low-molecular-weight inhibitors for HuR. *Nat Chem Biol* **3:** 508–515

Mesarovic MD, Sreenath SN, Keene JD (2004) Search for organising principles: understanding in systems biology. *Syst Biol (Stevenage)* **1:** 19–27

Mi H, Guo N, Kejariwal A, Thomas PD (2007) PANTHER version 6: protein sequence and function evolution data with expanded representation of biological pathways. *Nucleic Acids Res* **35:** D247–D252

Mili S, Steitz JA (2004) Evidence for reassociation of RNA-binding proteins after cell lysis: implications for the interpretation of immunoprecipitation analyses. *RNA (New York, NY)* **10:** 1692–1694

Ming XF, Stoecklin G, Lu M, Looser R, Moroni C (2001) Parallel and independent regulation of interleukin-3 mRNA turnover by phosphatidylinositol 3-kinase and p38 mitogen-activated protein kinase. *Mol Cell Biol* **21:** 5778–5789

Morris AR, Mukherjee N, Keene JD (2008) Ribonomic analysis of human Pum1 reveals cis-trans conservation across species despite evolution of diverse mRNA target sets. *Mol Cell Biol* **28:** 4093–4103

Morris AR, Mukherjee N, Keene JD (2009) Systematic analysis of posttranscriptional gene expression. *WIREs Systems Biol Med* doi:10.1002/wsbm.54

Newman JR, Ghaemmaghami S, Ihmels J, Breslow DK, Noble M, DeRisi JL, Weissman JS (2006) Single-cell proteomic analysis of S. cerevisiae reveals the architecture of biological noise. *Nature* **441:** 840–846

Papadaki O, Milatos S, Katsanou V, Grammenoudi S, Mukherjee N, Keene JD, Kontoyiannis D (2009) Control of thymic T-cell maturation, deletion and egress by the RNA-binding protein HuR. *J Immunol* **182:** 6779–6788

Pearson K (1894) Contributions to the mathematical theory of evolution. *Philos Trans R Soc Lond* **185:** 71–110

Penalva LO, Burdick MD, Lin SM, Sutterluety H, Keene JD (2004) RNA-binding proteins to assess gene expression states of co-cultivated cells in response to tumor cells. *Mol Cancer* **3:** 24

Pryzbylkowski P, Obajimi O, Keen JC (2007) Trichostatin A and 5 Aza-2′ deoxycytidine decrease estrogen receptor mRNA stability in ER positive MCF7 cells through modulation of HuR. *Breast Cancer Res Treat* **111:** 15–25

Pullmann Jr R, Kim HH, Abdelmohsen K, Lal A, Martindale JL, Yang X, Gorospe M (2007) Analysis of turnover and translation regulatory RNA-binding protein expression through binding to cognate mRNAs. *Mol Cell Biol* **27:** 6265–6278

Shaw G, Kamen R (1986) A conserved AU sequence from the 3′ untranslated region of GM-CSF mRNA mediates selective mRNA degradation. *Cell* **46:** 659–667

Silanes IL, Gorospe M, Taniguchi H, Abdelmohsen K, Srikantan S, Alaminos M, Berdasco M, Urdinguio RG, Fraga MF, Jacinto FV, Esteller M (2009) The RNA-binding protein HuR regulates DNA methylation through stabilization of DNMT3b mRNA. *Nucleic Acids Res* **37:** 2658–2671

Staal FJ, Clevers HC (2003) Wnt signaling in the thymus. *Curr Opin Immunol* **15:** 204–208

Stoecklin G, Tenenbaum SA, Mayo T, Chittur SV, George AD, Baroni TE, Blackshear PJ, Anderson P (2008) Genome-wide analysis identifies interleukin-10 mRNA as target of tristetraprolin. *J Biol Chem* **283:** 11689–11699

Subramanian A, Tamayo P, Mootha VK, Mukherjee S, Ebert BL, Gillette MA, Paulovich A, Pomeroy SL, Golub TR, Lander ES, Mesirov JP (2005) Gene set enrichment analysis: a knowledge-based approach for interpreting genome-wide expression profiles. *Proc Natl Acad Sci USA* **102:** 15545–15550

Tenenbaum SA, Carson CC, Lager PJ, Keene JD (2000) Identifying mRNA subsets in messenger ribonucleoprotein complexes by using cDNA arrays. *PNAS* **97:** 14085–14090

Thiele A, Nagamine Y, Hauschildt S, Clevers H (2006) AU-rich elements and alternative splicing in the beta-catenin 3′UTR can influence the human beta-catenin mRNA stability. *Exp Cell Res* **312:** 2367–2378

Tiruchinapalli DM, Caron MG, Keene JD (2008) Activity-dependent expression of ELAV/Hu RBPs and neuronal mRNAs in seizure and cocaine brain. *J Neurochem* **107:** 1529–1543

Townley-Tilson WH, Pendergrass SA, Marzluff WF, Whitfield ML (2006) Genome-wide analysis of mRNAs bound to the histone stem-loop binding protein. *RNA (New York, NY)* **12:** 1853–1867

Ule J, Jensen K, Mele A, Darnell RB (2005) CLIP: a method for identifying protein-RNA interaction sites in living cells. *Methods (San Diego, Calif)* **37:** 376–386

Wang JG, Collinge M, Ramgolam V, Ayalon O, Fan XC, Pardi R, Bender JR (2006) LFA-1-dependent HuR nuclear export and cytokine mRNA stabilization in T cell activation. *J Immunol* **176:** 2105–2113

Wang W, Caldwell MC, Lin S, Furneaux H, Gorospe M (2000a) HuR regulates cyclin A and cyclin B1 mRNA stability during cell proliferation. *EMBO J* **19:** 2340–2350

Wang W, Furneaux H, Cheng H, Caldwell MC, Hutter D, Liu Y, Holbrook N, Gorospe M (2000b) HuR regulates p21 mRNA stabilization by UV light. *Mol Cell Biol* **20:** 760–769

Wang W, Yang X, Cristofalo VJ, Holbrook NJ, Gorospe M (2001) Loss of HuR is linked to reduced expression of proliferative genes during replicative senescence. *Mol Cell Biol* **21:** 5889–5898

Wang W, Yang X, Kawai T, Lopez de Silanes I, Mazan-Mamczarz K, Chen P, Chook YM, Quensel C, Kohler M, Gorospe M (2004) AMP-activated protein kinase-regulated phosphorylation and acetylation of importin alpha1: involvement in the nuclear import of RNA-binding protein HuR. *J Biol Chem* **279:** 48376–48388

Wax S, Piecyk M, Maritim B, Anderson P (2003) Geldanamycin inhibits the production of inflammatory cytokines in activated macrophages by reducing the stability and translation of cytokine transcripts. *Arthritis Rheum* **48:** 541–550

Wilkinson DJ (2009) Stochastic modelling for quantitative description of heterogeneous biological systems. *Nat Rev* **10:** 122–133

Young DS, Hunter DR, Elmore RT, Xuan F, Hettmansperger TP, Thomas H (2007) The mixtools Package Version 0.2.0: Tools for Mixture Models. R Package Version 0.2.0. http://www.r-project.org